

COMPARISON BETWEEN DETAILED MODEL AND SIMPLIFIED MODELS OF A LI-ION BATTERY HEATED AT LOW TEMPERATURES

by

Zhiguo LEI and Jiawei ZHAI*

College of Mechanical and Electronic Engineering,
Fujian Agriculture and Forestry University, Fuzhou, Fujian, China

Original scientific paper
<https://doi.org/10.2298/TSCI220128175L>

With the development of hybrid electric vehicles and electric vehicles, more and more attention has been paid to Li-ion batteries. Since the charge-discharge performances of Li-ion batteries are affected by the temperature, an effective thermal management system is the key to solve the problem. Therefore, it is necessary to establish different simulation models to simulate the effects of the various thermal management systems. The prismatic pouch Li-ion batteries cell is composed of multiple cell units connected in parallel, to reduce the calculation, the simplified models are used to simulate the Li-ion batteries. In this paper, one detailed model and two simplified models are established to simulate temperature uniformity of heating Li-ion batteries cells, and heating methods are the self-heating Li-ion batteries structure heating method and the wide-line metal film heating method. The simulation results of the detailed model and two simplified models are compared and analyzed. The results show that there are difference between the detailed model and the two simplified models about temperature difference of the Li-ion batteries cell, and the two simplified models have the same simulation results. Finally, the simulation results of the detailed models with different footprint areas are compared. The comparison results show that different footprint areas have no effect on the simulation results for both the self-heating Li-ion batteries structure heating method and the wide-line metal film heating method.

Key words: *low temperature, battery heating method, 3-D heating model, Li-ion battery*

Introduction

Now, hybrid electric vehicles (HEV) and electric vehicles (EV) are considered as potential substitutes for gasoline and diesel vehicles, and the number of HEV and EV is increasing rapidly in the world. However, there are still some problems needing to be solved in HEV and EV. Especially for Li-ion batteries (LIB), they are a critical component in HEV and EV and sensitive to temperature. At high temperatures, the batteries life are shortened and the reliability are decreased, even probable explosion is caused for thermal runaway [1-7]. On the other hand, a low temperature environment will cause the charge and discharge performance of LIB to rapidly deteriorate [8-10]. Therefore, the thermal management system must have the ability to maintain the temperature of the LIB at the most suitable temperature.

* Corresponding author, e-mail: zjw2933795846@163.com

Many researchers are currently pursuing methods for efficiently heating or cooling LIB in different environments. Air-cooled is taken as an active thermal management, it is used in many HEV and EV for its advantages of simple and convenience [11, 12]. However, the effectiveness of air-cooled is not good, especially under the conditions of high charge and discharge rate and high ambient temperature. The passive thermal management of LIB that made use of PCM was presented [13-16], the PCM thermal management is able to control LIB to an optimal temperature with no need for extra cooling power, and even LIB are in high temperature ambient or work at high charge-discharge rates. Mohammadian and Zhang [17] present using pin-fin heat sinks to improve the effectiveness of air-cooled. Comparing with cooling, heating LIB was paid close attention in recent years. Despite all this, many effective heating methods have been presented, such as: alternating current (AC) heating method [18-21], liquid heating method [22, 23], wide line metal film heating method [24-27], and self-heating LIB heating method (SHLBHM) [28, 29], *etc.*

In order to further analyze the efficiency of thermal management system, temperature distribution of LIB heated or cooled, establishing relative simulation models is necessary. However, for LIB cell, it is composed of several different components, such as: anode, cathode, electrolyte, and separator. Besides, thickness of every component is very small, from 10-50 μm , and it is only a few thousandths of LIB cell thickness, and it is smaller than LIB cell length and width. Therefore, for simplified calculation, generally, the layered-structure of a LIB cell was taken as a homogeneous material. Furthermore, an unacceptable calculation time could be needed if simulation models are too complicated. However, there are still differences between simplified model and detailed model. In this study, in order to simulate the heating process of a prismatic soft-packed LIB at low temperatures, a 3-D transient heating model was established. In the transient heating model, the LIB cell is established in accordance with the real layer structure instead of a homogeneous material. This model is compared with simplified models by simulation results.



Figure 1. A disassembled prismatic pouch LIB cell

Problem statement

It is well known that the most prismatic pouch LIB cell is composed of multiple cell units connected in parallel. Figure 1 illustrates a disassembled prismatic pouch LIB cell. Every cell unit consists of anode, cathode, electrolyte and separator, as shown in fig. 2(a). Different capacities LIB cells include different number of cell units, as shown in fig. 2(b). In general, there are two typical simplified models of LIB cell. One is taking the whole LIB cell as a homogeneous material, and establishes a homogeneous block as a LIB cell. This simplified model is used in most researches. The another is taking the cell unit as a homogeneous material. The second simplified model is less used

unless the character of cell units is researched. However, no matter use which simplified model, cell unit is considered as a homogeneous material. Furthermore, temperature sensors cannot be placed inside battery cell, and simulation results of temperature inside battery cell cannot be verified by experiment data. Therefore, the outer surface temperatures of battery cell that are

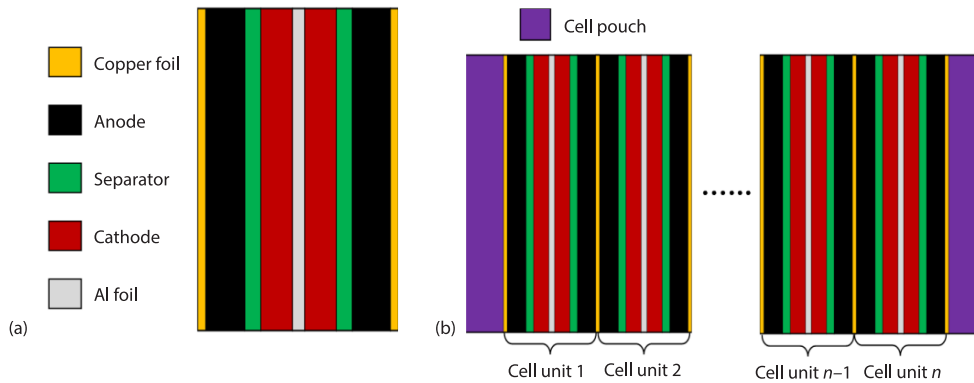


Figure 2. The structure of a cell unit (a) and LIB cell (b)

measured by temperature sensors are used to verify accuracy of the simplified models. Generally, if the simulation results of outer surface temperature of battery cell match well with the experiment data, the predicted inside temperature of battery cell is also considered as right. It seems to be feasible. However, a problem is ignored that the whole LIB cell is assumed to be a homogeneous material in simulation models. In fact, a LIB cell is composed of different materials, and these materials have their own thermal properties. Therefore, whether do this assumption affect the correct of the simulation results of inside temperature of battery cell. What differences are there between the simplified models and the models established according to the real structure of battery cell. The two questions should be considered seriously. In this study, simplified and detailed transient heating models of two heating methods of SHLBHM and wide-line metal film heating method (WLMFHM) was established, and simulation results of internal temperature of heated battery cells were compared. As shown in fig. 3(a), the SHLBHM is to place heating films at 1/4 and 3/4 of the battery thickness. In addition, the papers [28-31] describe the SHLBHM in detail. Then, as shown in fig. 3(b), the WLMFHM places two wide-line metal films on the two largest surfaces of the LIB. In addition, the papers [24-27] describe the WLMFHM in detail.

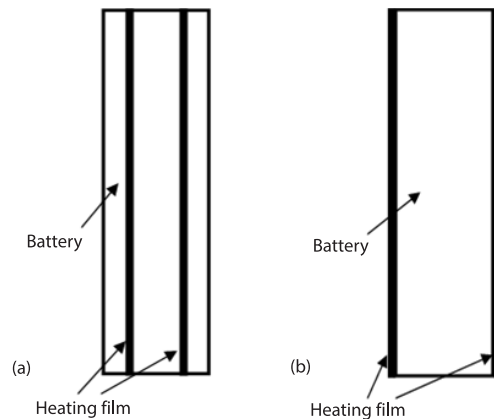


Figure 3. Location of heating films;
 (a) location of heating films in SHLBHM and
 (b) location of heating films in WLMFHM

In this work, the prismatic pouch LIB cell is using $\text{LiNi}_{0.6}\text{Co}_{0.2}\text{Mn}_{0.2}\text{O}_2$ as cathodes and Nippon Carbon as anodes. Each cell has a $152 \times 75 \text{ mm}^2$ footprint area and 10 Ah nominal capacity [30]. Without loss of generality, the transient heating model established and analysis results in this work can be used in any prismatic battery cell. The detailed transient heating models are established according to the structure of a LIB cell. Owing to the thickness of every material in cell unit is very thin, such as: the thickness of Anode is $48.7 \mu\text{m}$, and it is the thickest in cell unit, it is impossible to establish the detailed model of the whole LIB cell for an unacceptable calculation time. Therefore, the calculation must be reduced to an acceptable range. Firstly, in the thickness direction, because of the symmetry, the models can be established

according to half the thickness of battery cell, and amount of calculation reduces by half. Secondly, although the models can be established according to half the length and width of battery cell because of the symmetry, calculation time of models is still unacceptable. Since battery cell internal structure and temperature inside battery in the process of heating are focused, very small area from the center position of battery cell is taken to establish models. The small area is $20 \times 20 \mu\text{m}^2$, as shown in fig. 4. The whole battery cell is shown in fig. 4(a). Figure 4(b) shows the detailed model established according to the structure of battery cell, the length, width and thickness of the model are $20 \mu\text{m}$, $20 \mu\text{m}$ and half the thickness of battery cell, respectively. In order to appear the model, it is enlarged in fig. 4(b). For showing the structure of the detailed model, fig. 4(c) shows the enlarged image for certain position of the model. Furthermore, fig. 5(a) shows the model of SHLBHM, and fig. 5(b) shows the model of WLMFHM. In fact, the difference between models of two heating methods is the position of heating film. In this work, the simulation results of detailed models and simplified models about temperature inside battery cell are compared, and the differences between the detailed models and simplified models are revealed.

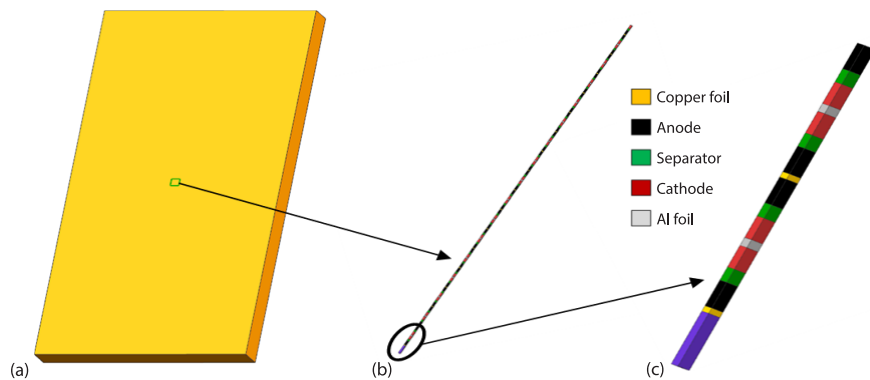


Figure 4. (a) The whole battery, (b) the detailed model established according to the structure of battery cell, and (c) the enlarged image for certain position of the detailed model

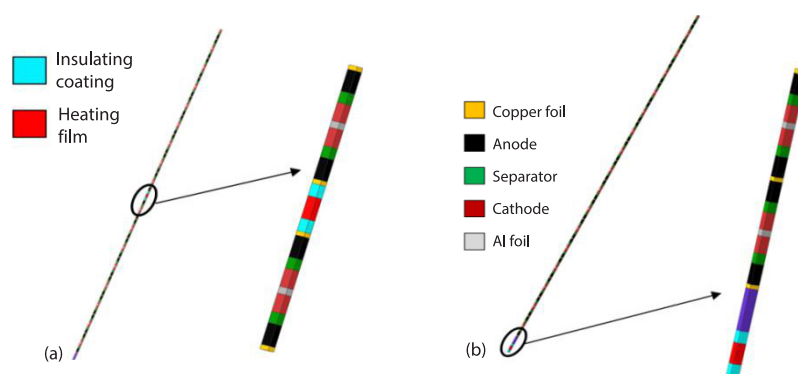


Figure 5 (a) The detailed model of SHLBHM and (b) the detailed model of WLMFHM

Numerical solution

In this work, the transient 3-D conductive heat transfer equation has been used [32]. Since the battery cell and the heating element are an opaque system, the radiant heat transfer between them is negligible:

$$\rho C_p \frac{\partial T}{\partial t} = \frac{\partial}{\partial x} \left(k_x \frac{\partial T}{\partial x} \right) + \frac{\partial}{\partial y} \left(k_y \frac{\partial T}{\partial y} \right) + \frac{\partial}{\partial z} \left(k_z \frac{\partial T}{\partial z} \right) + Q \quad (1)$$

In this work, it is assumed that the material properties are isotropic, so the values of k_x , k_y , and k_z are equal. This work is based on the thermal performance of LIB introduced by Yang *et al.* [29].

Among eq. (1), Q is the heat source, which represents the heating rate per unit volume. The heat source can be calculated:

$$Q = \frac{(E_{oc} - E)I}{V_{cell}} + \frac{EI}{V_{heatingfilm}} \quad (2)$$

These data of E_{oc} , E , I , V_{cell} , and $V_{heatingfilm}$ are from Zhang *et al.* [31].

The boundary conditions are given:

$$-k \frac{\partial T}{\partial n} \Big|_{\Gamma} = h_c (T_s - T_{amb}) \quad (3)$$

The term h_c in eq. (3) represents the convective heat transfer coefficient. In this study, the LIB in the incubator is in a natural-convection environment. The h_c can be calculated:

$$h_c = f_1 \left(\frac{|T_s - T_{amb}|}{P} \right)^n \quad (4)$$

These data of P , f_1 , and n can be determined in Chen [33].

Results and discussion

Transient heating models of SHLBHM

In this section, simulation results of the detailed and simplified transient heating models of SHLBHM are compared. Figure 6 shows temperature distribution curves of a LIB heated by SHLBHM at $-20\text{ }^{\circ}\text{C}$ for 12.5 seconds. The three temperature distribution curves in fig. 6 are simulation results of a detailed and two simplified transient heating models, respectively. For two simplified transient heating models, in the first simplified transient heating model, the cell unit is considered as a homogeneous material, in the second simplified transient heating model, the whole battery cell is considered as a homogeneous material. The first simplified model is named simplified Model I, and the second simplified model is named simplified Model II. From fig. 6, it is clear that the simulation results of simplified Model I and Model II is almost same. However, the simulation results of the detailed model are different with simplified Model I and Model II. The highest temperature in the detailed model is lower than that of simplified Model I or Model II, and the lowest temperature in the detailed model is higher than that of simplified Model I or Model II. Therefore, the temperature difference of battery cell in the detailed model is smaller than that of simplified Model I or Model II. The highest, lowest, average temperature and standard deviation are shown in tab. 1. The simulation temperature difference of the battery cell in the detailed model is smaller by 3.4 K than that of simplified Model I or Model II. What's more, the heating film and insulation coating are not belong to LIB cell, and temperature of the heating film and insulation coating cannot represent the temperature

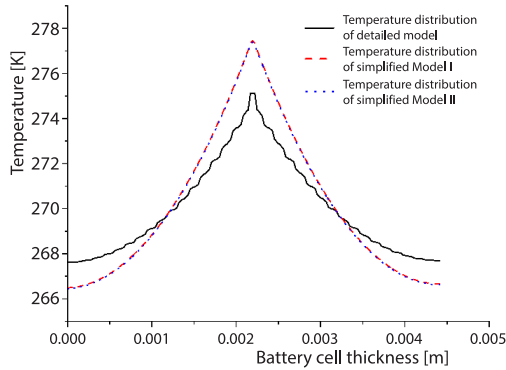


Figure 6. The temperature distribution curves of a LIB heated by SHLBHM at $-20\text{ }^{\circ}\text{C}$ for 12.5 seconds

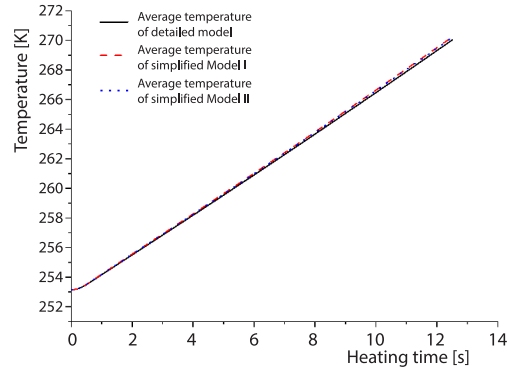


Figure 7. Three average temperature curves of a battery cell in three models during heating by SHLBHM

of LIB cell. If the temperature of the heating film and insulation coating is not considered, the simulation temperature difference of battery cell in the detailed model becomes smaller. For average temperature of battery cell, simulation results of three models are almost same. Figure 7 shows three average temperature curves of a battery cell in three models during heating, and three curves almost overlap. Then, fig. 8 shows three outlet surface average temperature curves of LIB cell in three models during heating at $-20\text{ }^{\circ}\text{C}$. Although, there are differences between the detailed model and two simplified models about outlet surface average temperature of a LIB cell, the maximum difference is near 1.1 K. Therefore, through the aforementioned analysis, for SHLBHM, the main difference between the detailed model and the two simplified models is the temperature distribution inside the battery cell. The simulation results of the detailed model and the two simplified models are only slightly different in terms of the average temperature of the outlet surface of the LIB, while the simulation results of the two simplified models are almost the same.

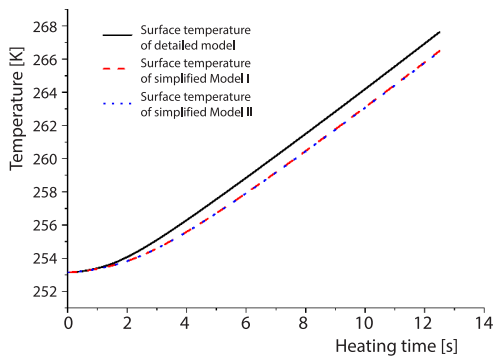


Figure 8. Three outlet surface average temperature curves of LIB cell in three models during heating by SHLBHM

Table 1. The maximum, minimum, average temperature [K], and the standard deviation of battery cell in different models during heating by SHLBHM

	Detailed model	Simplified Model I	Simplified Model II	Detailed model does not include heating film and insulation coating	Simplified Model I does not include heating film and insulation coating	Simplified Model II does not include heating film and insulation coating
Maximum	275.13	277.44	277.38	274.37	277.04	276.97
Minimum	267.63	266.49	266.45	267.63	266.49	266.45
Difference	7.50	10.96	10.93	6.74	10.55	10.52
Average	270.03	270.23	270.18	269.91	270.06	270.01
St. Dev.	2.1248	3.2600	3.2519	2.0049	3.1041	3.0963

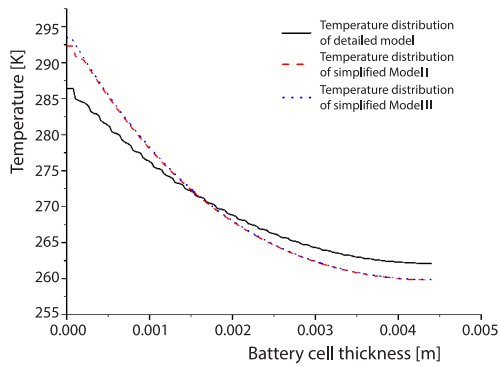


Figure 9. The temperature distribution curves of a LIB heated by WLMFHM at $-20\text{ }^{\circ}\text{C}$ for 12.5 seconds

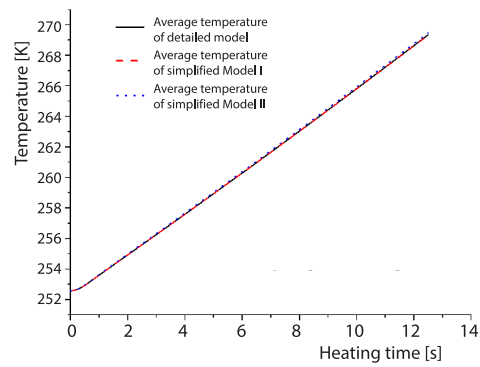


Figure 10. Three average temperature curves of a battery cell in three models during heating by WLMFHM

Table 2. The maximum, minimum, average temperature [K], and the standard deviation of battery cell in different models

	Detailed model	Simplified Model I	Simplified Model II	Detailed model does not include heating film and insulation coating	Simplified Model I does not include heating film and insulation coating	Simplified Model II does not include heating film and insulation coating
Maximum	286.44	292.33	293.52	284.95	290.86	292.49
Minimum	262.12	259.82	259.85	262.12	259.82	259.85
Difference	24.32	32.52	33.66	22.84	31.05	32.64
Average	269.95	269.93	270.09	269.55	269.38	269.51
St. Dev.	7.2793	9.8301	9.9875	6.8956	9.2991	9.4110

Transient heating models of WLMFHM

As in the previous section, the detailed and simplified heating models of the WLMFHM are established. In addition, the simulation results of the three models are compared. Figure 9 shows the temperature curves of a LIB using the WLMFHM at $-20\text{ }^{\circ}\text{C}$ for 12.5 seconds. Similar to the SHL-BHM, the cell temperature difference in the detailed model is smaller than the simplified Model I or Model II, and the cell temperature difference in the simplified Model I is the same as the simplified Model II. Table 2 lists the highest, lowest, average temperature and standard deviation. The simulation temperature difference of battery cell in the detailed model is smaller by 8-9 K than that of simplified Model I or Model II. If the temperature of the heating film and insulation coating is not considered, the simulation temperature difference of battery cell in the detailed model becomes smaller. Similarly, for average temperature of battery cell, simulation results of three models are almost same, as shown in fig. 10. However, for surface average temperature of battery cell, simulation results of detailed model is different from two simplified models. As is shown in fig. 11, surface average temperature of battery cell in simplified

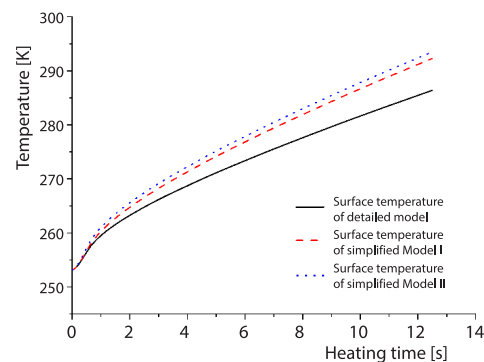


Figure 11. Three outlet surface average temperature curves of LIB cell in three models during heating by WLMFHM

Model II is higher 7.1 K than detailed model in the end of heating. And the difference of surface average temperature between simplified Model I and simplified Model II is very small.

Compare the detailed models with different footprint areas

In order to reduce the calculation of the detailed transient heating model, only $20 \times 20 \mu\text{m}^2$ area is taken from the center position of battery cell to detailed models. In this section, the different footprint areas affecting the simulation results of the detailed transient heating models of SHLBHM and WLMFHM are considered. The footprint area is increased from $20 \times 20 \mu\text{m}^2$ to $100 \times 100 \mu\text{m}^2$, and $200 \times 200 \mu\text{m}^2$, and the detailed models with $100 \times 100 \mu\text{m}^2$ and $200 \times 200 \mu\text{m}^2$ areas of SHLBHM and WLMFHM are established. Figure 12 shows temperature distribution simulation curves of the detailed transient heating models with $20 \times 20 \mu\text{m}^2$, $100 \times 100 \mu\text{m}^2$, and $200 \times 200 \mu\text{m}^2$ areas of a LIB heated by SHLBHM at -20°C for 12.5 seconds. It can be clearly seen that the different footprint areas have no effect on the simulation results of the temperature distribution of the LIB cell heated by SHLBHM. For

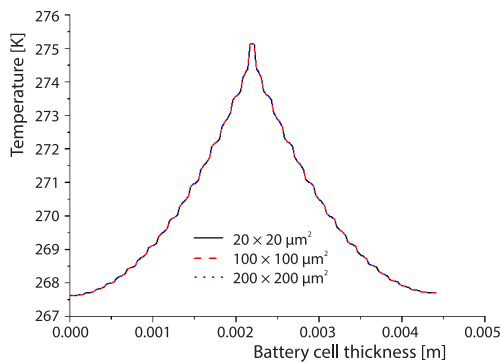


Figure 12. The temperature distribution simulation curves of the detailed transient heating models with three different footprint areas of a LIB heated by SHLBHM at -20°C for 12.5 seconds

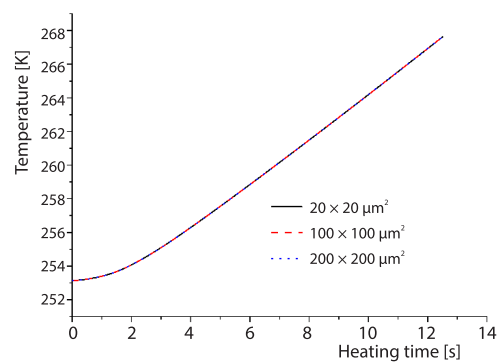


Figure 13. The average temperature curves of the detailed transient heating models with three different footprint areas of a LIB heated by SHLBHM at -20°C for 12.5 seconds

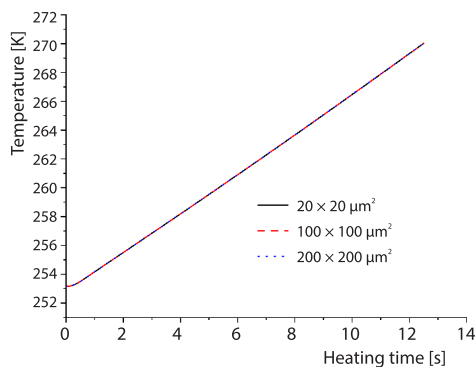


Figure 14. The surface average temperature curves of the detailed transient heating models with three different footprint areas of a LIB heated by SHLBHM at -20°C for 12.5 seconds

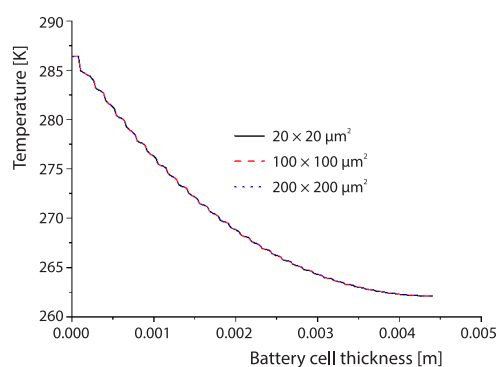


Figure 15. The temperature distribution simulation curves of the detailed transient heating models with three different footprint areas of a LIB heated by WLMFHM at -20°C for 12.5 seconds

the average temperature of the heated LIB, the same conclusion can be obtained, as shown in fig. 13 and fig. 14. Therefore, the different footprint areas have no effect on the simulation results of the detailed transient heating model of SHLBHM. For WLMFHM, the different footprint areas also have no effect on the simulation results of the detailed transient heating model, as shown in figs. 15 and 16. Therefore, for both SHLBHM and WLMFHM, the footprint area has no effect on the simulation results of the detailed transient heating model.

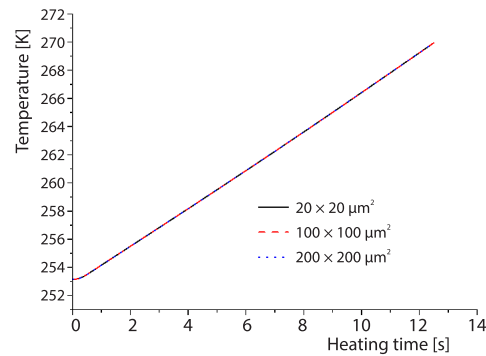


Figure 16. The average temperature curves of the detailed transient heating models with three different footprint areas of a battery cell during heating by WLMFHM at $-20\text{ }^{\circ}\text{C}$ for 12.5 seconds

Conclusion

In the present study, one detail and two simplified 3-D transient heating models of a LIB cell heated by SHLBHM and WLMFHM have been established. The simulation results of different transient heating models have been compared and analyzed. In the form of SHLBHM, the temperature difference of the cells in the detailed model is smaller than that of the simplified Model I or Model II. The average temperatures of the battery cell in the detailed and two simplified models are similar, the surface average temperature of a LIB, there is only a little difference between the simulation results of the detailed model and two simplified models, two simplified models have the same simulated results. For WLMFHM, the similar conclusions have been drawn. Therefore, the two simplified models can be employed to simulate the average temperature and outlet surface average temperature of a heated LIB cell. If the two simplified models are employed to simulate the temperature distribution inside battery cell, the difference between the detailed model and simplified models should be considered. In the case of high precision, it is best to choose the detailed model to simulate the temperature distribution inside battery cell. At the same time, the detailed models with different footprint areas have been compared. The comparison results show that different footprint areas have no effect on the simulation results of the detailed transient heating models of a heated LIB cell.

Acknowledgment

This work was supported by the Natural Science foundation of Fujian Province (2019J01405).

Nomenclature

C_p – battery constant pressure heat capacity [Jkg⁻¹K⁻¹]
 E – cell working voltage [V]
 E_o – open-circuit potential of LIB cell [V]
 f_i – coefficient of eq. (4) [Wmⁿ⁻²K⁻ⁿ⁻¹]
 h_c – convective heat transfer coefficient
 I – cell current [A]
 k – thermal conductivity [Wm⁻¹K⁻¹]
 n – coefficient of eq. (4)
 P – length of the surface of a LIB cell [m]
 Q – heating rate per unit volume [Wm⁻³]

T – battery temperature [°C]
 T_{amb} – ambient temperature [K]
 T_s – surface temperature of the LIB [K]
 V_{cell} – cell volume [m³]
 $V_{heatingfilm}$ – heating film volume [m³]

Greek symbol

ρ – battery density [kgm⁻³]

Subscript

X – X -direction

Y – Y-direction
Z – Z-direction

Acronyms

AC – alternating current
EV – electric vehicles

HEV – hybrid electric vehicles
LIB – Li-ion battery
SHLBHM – self-heating Li-ion battery structure heating method
WLMFHM – wide-line metal film heating method

References

- [1] Lisbona, D., Snee, T., A Review of Hazards Associated with Primary Lithium and Lithium-Ion Batteries, *Process Safety and Environmental Protection*, 89 (2011), 6, pp. 434-442
- [2] Feng, Z. C., Zhang, Y., Safety Monitoring of Exothermic Reactions Using Time Derivatives of Temperature Sensors, *Applied Thermal Engineering*, 66 (2014), 1-2, pp. 346-354
- [3] Fathabadi, H., A Novel Design Including Cooling Media for Lithium-Ion Batteries Pack Used in Hybrid and Electric Vehicles, *Journal of Power Sources*, 245 (2014), Jan., pp. 495-500
- [4] Duh, Y.-S., et al., Characterization on the Thermal Runaway of Commercial 18650 Lithium-Ion Batteries Used in Electric Vehicle, *Journal of Thermal Analysis and Calorimetry*, 127 (2016), 1, pp. 983-993
- [5] Lee, C. H., et al., A Study on Effect of Lithium Ion Battery Design Variables Upon Features of Thermal-Runaway Using Mathematical Model and Simulation, *Journal of Power Sources*, 293 (2015), Oct., pp. 498-510
- [6] Ning, F., et al., Simulation Study on Thermal Runaway Behaviors of Lithium-Ion Batteries, *Chinese Journal of Power Supply*, 44 (2020), 08, pp. 1102-1104
- [7] Chen, J., et al., Experimental Study on Safety of Automotive NCM Battery under Different Abuse Conditions, *Automotive Engineering*, 42 (2020), 20, pp. 66-73
- [8] Lei, Z., et al., A Study on the Low-Temperature Performance of Lithium-Ion Battery for Electric Vehicles, *Automotive Engineering*, 35 (2013), 10, pp. 927-933
- [9] Lei, Z., et al., Research on Thermal Characteristics of EV Lithium-Ion Battery, *Chinese Journal of Power Supply*, 54 (2014), 4, pp. 83-87
- [10] Smart, M. C., et al., Improved Low-Temperature Performance of Lithium-Ion Cells with Quaternary Carbonate-Based Electrolytes, *Journal of Power Sources*, 119-121 (2003), June, pp. 349-358
- [11] Park, H., A Design of Air-Flow Configuration for Cooling Lithium Ion Battery in Hybrid Electric Vehicles, *Journal of Power Sources*, 239 (2013), Oct., pp. 30-36
- [12] Wang, Y., et al., Optimization of an Air-Based Thermal Management System for Lithium-Ion Battery Packs, *Journal of Energy Storage*, 44 (2021), Part A, 103314
- [13] Duan, X., Naterer, G. F., Heat Transfer in Phase Change Materials for Thermal Management of Electric Vehicle Battery Modules, *International Journal of Heat and Mass Transfer*, 53 (2010), 23-24, pp. 5176-5182
- [14] Ling, Z., et al., A Hybrid Thermal Management System for Lithium Ion Batteries Combining Phase Change Materials with Forced-Air Cooling, *Applied Energy*, 148 (2015), June, pp. 403-409
- [15] Wang, Y., et al., Performance Investigation of a Passive Battery Thermal Management System Applied with Phase Change Material, *Journal of Energy Storage*, 35 (2021), Mar., 102279
- [16] Joshy, N., et al., Experimental Investigation of the Effect of Vibration on Phase Change Material (PCM) Based Battery Thermal Management System, *Journal of Power Sources*, 450 (2020), Feb., 227717
- [17] Mohammadian, S. K., Zhang, Y., Thermal Management Optimization of an Air-Cooled Li-Ion Battery Module Using Pin-Fin Heat Sinks for Hybrid Electric Vehicles, *Journal of Power Sources*, 273 (2015), Jan., pp. 431-439
- [18] Stuart, T.B.A., Hande, A., The HEV Battery Heating Using AC Currents, *Journal of Power Sources*, 129 (2004), 2, pp. 368-378
- [19] Zhang, J., et al., Internal Heating of Lithium-Ion Batteries Using Alternating Current Based on the Heat Generation Model in Frequency Domain, *Journal of Power Sources*, 273 (2015), Jan., pp. 1030-1037
- [20] Zhu, J., et al., Experimental Investigations of an AC Pulse Heating Method for Vehicular High Power Lithium-Ion Batteries at Subzero Temperatures, *Journal of Power Sources*, 367 (2017), Nov., pp. 145-157
- [21] Shang, Y., et al., Modelling and Analysis of High-Frequency Alternating-Current Heating for Lithium-Ion Batteries under Low-Temperature Operations, *Journal of Power Sources*, 450 (2020), Feb., 227435
- [22] Liu, J., et al., Thermal Characteristics of Power Battery Pack with Liquid-Based Thermal Management, *Applied Thermal Engineering*, 164 (2020), Jan., 114421
- [23] Wu, W., et al., A Critical Review of Battery Thermal Performance and Liquid Based Battery Thermal Management, *Energy Conversion and Management*, 182 (2019), Feb., pp. 262-281

- [24] Lei, Z., et al., Preheating Method of Lithium-Ion Batteries in an Electric Vehicle, *Journal of Modern Power Systems and Clean Energy*, 3 (2015), 2, pp. 289-296
- [25] Lei, Z., et al., Low-Temperature Performance and Heating Method of Lithium Battery in Electric Vehicle, *Journal of Beijing University of Technology*, 39 (2013), 9, pp. 1399-1405
- [26] Lei, Z., et al., Temperature Uniformity of a Heated Lithium-Ion Battery Cell in Cold Climate, *Applied Thermal Engineering*, 129 (2018), Jan., pp. 148-154
- [27] Lei, Z., et al., Improving Temperature Uniformity of a Lithium-Ion Battery by Intermittent Heating Method in Cold Climate, *International Journal of Heat and Mass Transfer*, 121 (2018), June, pp. 275-281
- [28] Wang, C.Y., et al., Lithium-Ion Battery Structure that Self-Heats at Low Temperatures, *Nature*, 529 (2016), 7587, pp. 515-8
- [29] Yang, X.-G., et al., Computational Design and Refinement of Self-Heating Lithium Ion Batteries, *Journal of Power Sources*, 328 (2016), Oct., pp. 203-211
- [30] Wang, C.-Y., et al., A Fast Rechargeable Lithium-Ion Battery at Subfreezing Temperatures, *Journal of The Electrochemical Society*, 163 (2016), 9, pp. A1944-A1950
- [31] Zhang, G., et al., Rapid Self-Heating and Internal Temperature Sensing of Lithium-Ion Batteries at Low Temperatures, *Electrochimica Acta*, 218 (2016), Nov., pp. 149-155
- [32] Wang, Q.-K., et al., Decoupling Parameter Estimation Strategy Based Electrochemical-Thermal Coupled Modelling Method for Large Format Lithium-Ion Batteries with Internal Temperature Experimental Validation, *Chemical Engineering Journal*, 424 (2021), Nov., 130309
- [33] Chen, S.C., et al., Thermal Analysis of Lithium-Ion Batteries, *Journal of Power Sources*, 140 (2005), 1, pp. 111-124,